THE AMERICAN MINERALOGIST, VOL. 56, MAY-JUNE, 1971

ORIENTATION OF EXSOLUTION LAMELLAE IN CLINOPYROXENES AND CLINOAMPHIBOLES: CONSIDERATION OF OPTIMAL PHASE BOUNDARIES

PETER ROBINSON AND HOWARD W. JAFFE, *Department of Geology, University of Massachusetts, Amherst, Massachusetts, 01002*

MALCOLM ROSS, *U. S. Geological Survey, Washington, D. C. 20242*

AND

CORNELIS KLEIN, JR., *Department of Geological Sciences, Harvard University, Cambridge, Mass. 02138*

ABSTRACT

Microscopic observations of clinopyroxene and clinoamphibole exsolution lamellae in clinopyroxene and clinoamphibole hosts, referred to space groups $C2/c$ and $I2/m$ respectively, show the lamellae are not usually oriented parallel to (001) and (100) as commonly believed, even though X-ray single crystal photographs usually suggest host and lamellae share a common (001) or (100) lattice plane. Coexisting magnesioarfvedsonite and manganoan cummingtonite, described in detail here, show an extreme example with lamellae 16° from (001) in the acute angle β and 6° from (100) in the obtuse angle β.

Two-dimensional evaluation in (010) of measured lattices of exsolved clinopyroxenes and clinoamphiboles shows that the lamellae are parallel to generally irrational planes of dimensional best fit between the lattices at the time exsolution began. Best fit is achieved by slight relative rotation of the lattices, but in most natural examples this rotation is less than 10′ and not easily observed on X-ray photographs. Using augite and pigeonite as examples, the relative a and c dimensions of the lattice with the smaller β angle (AUG) and the lattice with the larger β angle (PIG) determine the positions of the lamellae as follows:

	"001" lamellae		*"100" lamellae*
$a_{AUG} > a_{PIG}$	in acute angle β	$c_{AUG} > c_{PIG}$	in acute angle β (acu)
$a_{AUG} < a_{PIG}$	in obtuse angle β	$c_{AUG} < c_{PIG}$	in obtuse angle β (obt)

So far three of the four possible combinations of relative a and c dimensions have been found in natural specimens.

Lattice parameters may have changed since the nucleation of lamellae, either at constant composition as a result of thermal contraction, decompression, or reversible polymorphic transitions, or with changing composition as a result of the exsolution itself or element fractionation between host and lamellae. An augite from the Duluth Gabbro ($\beta = 106°0'$) contains two sets of "001" lamellae, a late set at 111–115° that agrees with 114° predicted from present lattice parameters, and an earlier set at 108–109° that is a "fossil" from a previously existing set of lattice parameters. The angles of lamellae thus provide a tool for deciphering the temperature-pressure histories of pyroxenes and amphiboles.

INTRODUCTION

In many occurrences in igneous and metamorphic rocks clinopyroxenes and clinoamphiboles contain exsolution lamellae of a second clinopyrox-

ene or clinoamphibole, respectively. In clinopyroxenes these lamellae have been generally described as oriented parallel to (100) and (001) of the *C*-centered cell (Poldervaart and Hess, 1951). In early work on the structure of clinoamphiboles, in which the analogy with pyroxenes was emphasized (Warren, 1929), the clinoamphibole structure was referred to space group $I2/m$, directly analogous to the space group of clinopyroxene $C2/c$. On this basis exsolution lamellae in clinoamphibole would also be described as oriented parallel to (100) and (001) (Jaffe, Robinson, and Klein, 1968). More recently clinoamphiboles have been referred to space group $C2/m$, because the long established rules of space group nomenclature dictate this choice and on this basis exsolution lamellae in clinoamphiboles have been described as oriented parallel to (100) and $(\bar{1}01)$ (Ross, Papike, and Weiblen, 1968; Ross, Papike, and Shaw, 1969). Zussman (1959), Wyckoff (1968), and Jaffe, Robinson, and Klein (1968) have pointed out some of the confusion this dual system has caused.[1] Because we will be discussing properties common to both pyroxenes and amphiboles, we will refer to amphibole lattice parameters of the *I*-cell.[2] Except that a long-standing usage of the *C*-setting would be changed, a return to the original $I2/m$ nomenclature of Warren (1929) has very much to recommend it structurally, morphologically, and pedagogically.

X-ray single crystal photographs of many clinoamphiboles studied by ourselves and by others show one exsolved clinoamphibole oriented such that its (001) lattice plane lies parallel to the (001) lattice plane of the host, and commonly a second clinoamphibole oriented such that its (100) lattice plane lies parallel to the (100) lattice plane of the host (Ross, Papike, and Weiblen, 1968; Ross, Papike, and Shaw, 1969). Similar results have been obtained in X-ray single crystal photographs of clinopyroxenes (Bown and Gay, 1959, 1960; Morimoto and Tokonami, 1969).

Specimen 7A8BX, studied by us in detail (Jaffe, Robinson, and Klein, 1968) contains hornblende (space group $I2/m$) with cummingtonite exsolution lamellae and cummingtonite (space group $I2/m$) with horn-

[1] This discussion refers to non-primitive clinopyroxenes and clinoamphiboles. For primitive pyriboles there is a choice between two alternate primitive cells structurally and metrically similar to the *C*- and *I*-cells. Experiments (Prewitt, Papike, and Ross, 1970; Smyth, 1970) show the primitive structures on heating invert to *C*- or *I*-structures, the temperature of inversion depending on composition.

[2] The parameters of the two alternate lattices have the following relationships:

$$(1)\ a_I = \sqrt{a_C^2 + c_C^2 + 2a_C c_C \cos\beta_C}; \qquad (2)\ b_I = b_C; \qquad (3)\ c_I = c_C;$$

$$(4)\ \sin\beta_I = \frac{a_C \sin\beta_C}{a_I}; \qquad (5)\ \text{(to avoid square roots)}\ \tan\beta_I = \frac{a_C \sin\beta_C}{c_C - a_C \lvert\cos\beta_C\rvert}.$$

blende exsolution lamellae. X-ray single crystal photographs of both kinds of hosts (Ross, Papike, and Shaw, 1969, Table 6) show that each contains two sets of exsolution lamellae with the lattices of the lamellae oriented parallel to the (100) and (001) lattice planes of the host. According to the measured β angles of these amphiboles (Table 3) (001) lamellae in the hornblende should make an angle of 106°31′ with the c-crystallographic axis, and (001) lamellae in the cummingtonite should make an angle of 109°39′ with the c crystallographic axis. Such an orientation would obtain only if the composition planes of the lamellae are parallel to the (001) lattice planes of the host. Repeated observations in oils and in thin sections on the universal stage showed that the lamellae in hornblende appeared to make an angle of about 110° with the c-crystallographic axis and the lamellae in cummingtonite an angle of 112° with the c-crystallographic axis. We called attention to this discrepancy of about 3.5 degrees in the hornblende and 2.3 degrees in the cummingtonite, but could not explain it, although we did suggest the possibility that the β angles had been different under the P-T conditions of exsolution than at present. Subsequently we have observed additional examples in which these discrepancies are much larger and more easily measured.

A manganoan tremolite from the Wight Mine, Gouverneur Mining District, New York, contains exsolution lamellae of manganoan P-cummingtonite (Ross, Papike, and Weiblen, 1968; Ross, Papike, and Shaw, 1969). X-ray single crystal photographs show the lamellae have the (001) plane of their lattice oriented parallel to (001) in the lattice of the host. The β angle of the tremolite and hence the angle (001) exsolution lamellae would make with the c axis is 106°20′. However, the optically observed lamellae make an angle of about 114° with the c axis, giving a discrepancy of about 8°. In one grain from this specimen we have observed extremely fine lamellae that lie at a 5° angle to the c-crystallographic axis in the obtuse angle β (the trace of the lamellae directed between $+a$ and $+c$ such as shown in Figure 5, example 6).

Augite coexisting with ferrohypersthene from hornblende granulite facies rocks of the Hudson Highlands (Jaffe and Jaffe, 1971) contains three sets of exsolution lamellae (Fig. 1). One set oriented parallel to (100) we believe to be partly pigeonite because we have observed strongly inclined extinction in many cases, and partly hypersthene on the basis of an X-ray single crystal photograph (Table 5). The second set is pigeonite oriented so that the lamellae make an angle of 116° with the c-crystallographic axis, but, according to X-ray data, with the (001) lattice plane oriented parallel to the (001) lattice plane of the augite host. The β angle for the augite host is 105°55′, so that these pigeonite lamellae lie at a 10° angle to the (001) plane. The lamellae of the third set are very

FIG. 1. Photomicrograph of augite from pyroxene granulite, Hudson Highlands, New York (Jaffe and Jaffe, 1971). View normal to (010) showing three sets of exsolution lamellae (set text and Table 5). One set represented by the prominent continuous lamella (vertical) is oriented parallel to (100) of the host. A second set of fairly coarse lamellae lies at a 116° angle to the c-crystallographic axis. A third set of very fine lamellae lies in the acute angle β at 6° to the c-crystallographic axis. The coarsest lamellae are 1.0 μm thick.

fine and lie in the acute angle β at an angle of about 6° to the c-crystallographic axis. On the basis of the X-ray photograph we believe these lamellae are also pigeonite with the (100) lattice plane parallel to (100) of the host. A very similar augite in mafic anorthosite from Cascade Mountain, Mount Marcy quadrangle, New York, contains the same three sets of lamellae, including a second set that lies at a 115° angle to the c-crystallographic axis.

Recently one of us discovered a specimen with coexisting amphiboles having lamellae with angular relationships even more extreme than any

of those described above. Because of its unusual nature and pertinence to the subject of this paper, we have taken the space here to record its optical properties, lattice parameters, and chemistry.

Exsolution Lamellae in Coexisting Magnesioarfvedsonite and Manganoan Cummingtonite

The occurrence of the amphibole pair manganoan magnesioarfvedsonite-manganoan cummingtonite was described by Klein (1966 and 1968; assemblage no. 5) from the metamorphosed Wabush Iron Formation in Southwestern Labrador, Canada. The sodic amphibole was then imprecisely identified as magnesioriebeckite. Since then this same assemblage, which is the only one reported in the literature of a sodium amphibole coexisting with an iron-magnesium amphibole, has been studied in greater detail. Not only do the two phases coexist, but both contain two sets of lamellae of probable exsolution origin similar to those in amphiboles described above. The assemblage in which the two amphiboles occur consists of the following minerals: manganoan magnesioarfvedsonite (50 percent), manganoan cummingtonite (15 percent), specularite (30 percent), magnesian rhodonite (4 percent) and a trace of talc. The rhodonite contains 14 weight percent MgO and 4.6 weight percent FeO which recalculates to a composition: $Fe_{0.15}Mg_{0.83}Mn_{0.87}Ca_{0.07}Si_{2.04}O_6$ (Klein, 1966).

In thin section the two amphiboles occur most commonly as closely intergrown, independent subhedral grains, both exhibiting numerous fine closely spaced lamellae that are only visible at high magnification and best under crossed nicols. In a few large grains magnesioarfvedsonite forms a rim around a central core of manganoan cummingtonite. The magnesioarfvedsonite can be distinguished from the colorless cummingtonite by its light yellow color and anomalous blue and brown interference colors. The optical parameters for both amphiboles determined in oils on a spindle stage are given in Table 1. Because the γ and β indices are essentially the same for both amphiboles the lamellae are only visible on an (010) section which allows determination of α and γ indices. On (100), which permits the determination of γ and β indices, the lamellae cannot be seen.

One set of lamellae, less than 1 μm thick, is oriented at about a 6° angle to the *c*-crystallographic axis as determined from traces of the {110} cleavage. A second set of lamellae about 1 μm thick lies at angles of about 123° and 125° to the *c*-crystallographic axis of magnesioarfvedsonite and manganoan cummingtonite hosts respectively. Because the thin lamellae lie in the obtuse angle between the thick lamellae and the *c*-crystallographic axis, the angle between the two sets of lamellae is about 117°

TABLE 1. OPTICAL AND X-RAY PARAMETERS FOR MANGANOAN MAGNESIO-ARFVEDSONITE AND MANGANOAN CUMMINGTONITE

	Magnesioarfvedsonite	*Manganoan Cummingtonite*
Optical Properties		
γ	1.650 ± .001	1.650 ± .001
β	1.643 ± .001	1.644 ± .001
α	1.638 ± .001	1.628 ± .001
$\gamma-\alpha$	0.012	0.022
$Z \wedge c$	39° ± 1°	22° ± 1°
2V (calc)	80°+	63°−
$c \wedge$ thicker exsolution lamellae	123° ± 1°	125° ± 1°
$c \wedge$ thinner exsolution lamellae	6° ± 1°	6° ± 1°
Angle between thinner and thicker lamellae	117° ± 1°	119° ± 1°
Color	very pale yellow; not pleochroic; anomalous blue and brown interference colors.	colorless
Unit Cell Parameters[1]		
Space Group $C2/m$		
a	9.885 ± .005 Å	9.620 ± .002 Å
b	18.006 ± .006 Å	18.062 ± .002 Å
c	5.295 ± .004 Å	5.314 ± .002 Å
β	104.04° ± .05°	102.78° ± .02°
V	914.23 ± .83 Å^3	900.51 ± .33 Å^3
Space Group $I2/m$ (calculated)		
a	10.018 Å	9.907 Å
β	106°49′	108°45′

[1] Based on slow scan X-ray diffractometer powder patterns (goniometer speed $\frac{1}{4}$° per minute, chart speed $\frac{1}{2}$ inch per minute) in ascending and descending modes, using high purity silicon as an internal standard. Parameters calculated using a least squares refinement program (Burnham, 1962) from 15–17 unambiguously indexed diffraction lines between 20° and 80° 2θ (CuK$\bar{\alpha}$).

and 119° in the magnesioarfvedsonite and cummingtonite hosts respectively. These features are illustrated in Figures 2 and 3. Note in Figure 3 that when the two hosts are joined along a plane parallel to the thicker exsolution lamellae their *c*-crystallographic axes are not parallel but make an angle of about 2° with each other (see Jaffe, Robinson, and Klein, 1968, Fig. 2).

X-ray single crystal precession photographs of both hosts show that

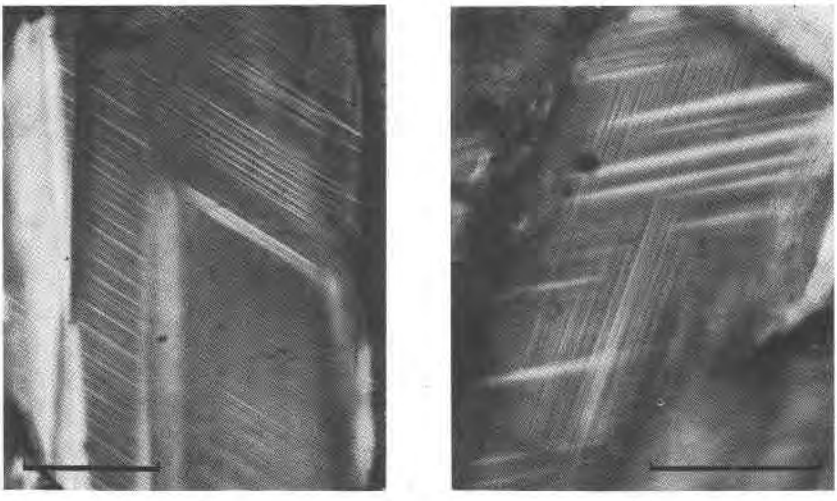

(A) (B)

FIG. 2. Photomicrographs of magnesioarfvedsonite and manganoan cummingtonite from the Wabush Iron Formation, Labrador under crossed nicols. A) Composite grain of cummingtonite and magnesioarfvedsonite (lower right corner) showing abundant thicker lamellae and a few thin lamellae (left side). B) Magnesioarfvedsonite grain at extinction showing two illuminated sets of cummingtonite exsolution lamellae. The thinner lamellae lie in the obtuse angle between the thicker lamellae and the *c*-crystallographic axis. Length of scale bars 50 μm.

the lattices of the hosts and of the lamellae are oriented most closely along (001) and (100). The β angles of the two hosts (Table 1) show that planes parallel to (001) make an angle of 106°49′ and 108°45′ with the *c*-crystallographic axes of magnesioarfvedsonite and cummingtonite respectively. The optically observed lamellae make angles of 123° and 125° with the *c*-axes, giving a discrepancy of 16° in each case. Obviously none of the composition planes of the lamellae can be described as parallel to (001) or (100) on the basis of the present lattice parameters.

The chemical composition of both amphiboles was determined on a polished thin section with an electron probe (ARL-EMX) using well analysed homogeneous amphibole standards and a reduction procedure previously described (Klein, 1968). Because of the lamellae it is difficult to locate one-phase amphibole areas for analysis. In the original analyses (Klein, 1966 and 1968) the chemical contribution of lamellae to the analysis of either amphibole was not fully taken into account. This time, every effort was made to reduce the possible contribution from enclosed and neighboring lamellae by careful optical location under the electron beam, by continuous X-ray monitoring of Mn K$\bar{\alpha}$ (Mn is a very large compo-

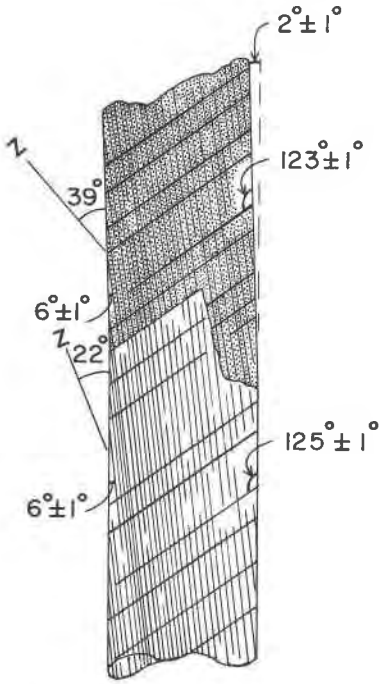

FIG. 3. Diagram of a grain of manganoan cummingtonite (white) and magnesioarfvedsonite (stippled) in contact along a plane parallel to one of the two sets of exsolution lamellae.

nent in the cummingtonite and smaller in the magnesioarfvedsonite) and by using a small electron beam. These analyses are given in Table 2, together with a complete wet chemical analysis of a bulk sample of approximately 80 percent magnesioarfvedsonite and 20 percent cummingtonite.

The fractionation of MnO, CaO, Na_2O, and K_2O is very pronounced between the two phases. The Na_2O content of the cummingtonite is larger than is generally present in such Fe-Mg amphiboles. Klein (1968) reported values of 0.2 weight percent Na_2O in metamorphic and 0.4 weight percent Na_2O in volcanic cummingtonites coexisting with hornblende. It is likely that the 1.1 weight percent value for Na_2O (Table 2, analysis 3) is high because of the contribution of fine magnesioarfvedsonite lamellae to the cummingtonite analyses. The K_2O fractionation is especially pronounced. The potassium in the magnesioarfvedsonite is undoubtedly housed only in the *A* site (Papike, Ross, and Clark, 1969), as is the very small amount of K in the cummingtonite.

Although the amounts of ferric iron could not be determined in the individual amphiboles, the wet analysis of the bulk amphibole sample

TABLE 2. CHEMICAL ANALYSES AND IONIC RATIOS FOR MAGNESIO-ARFVEDSONITE AND MANGANOAN CUMMINGTONITE

(1) Wet chemical analysis of bulk sample of approximately 80 percent magnesioarfvedsonite and 20 percent cummingtonite. Analyst: Jun Ito. FeO not detected; if present probably less than 0.5 weight per cent.
(2) Electron probe determination of individual magnesioarfvedsonite. n.d. = not detected. Total Fe recalculated as Fe_2O_3 only.
(3) Electron probe determination of individual manganoan cummingtonite. n.d. = not detected. Total Fe recalculated as Fe_2O_3 only.

	(1)	(2)	(3)	Recalculated on basis of 23 oxygens		
SiO_2	55.32	54.9	55.8		(2)	(3)
TiO_2	0.00	n.d.	n.d.	Si	7.890	8.000
Al_2O_3	0.10	0.1	0.1	Al	.016	—
Fe_2O_3	6.86	8.3	2.3	Fe^{3+}	.094	—
				Σ (tet.)	8.000	8.000
FeO	n.d.	0	0			
MnO	7.65	6.0	15.3	Si	—	.010
MgO	18.18	17.6	20.8	Al	—	.016
CaO	2.11	2.3	0.7	Fe^{3+}	.804	.252
Na_2O	4.65	5.7	1.1	Mg	3.770	4.450
K_2O	1.97	2.2	0.1	Mn^{2+}	.426	.272
				Σ [*M*(1–3)]	5.000	5.000
$H_2O(+)$	2.98					
$H_2O(-)$	.50			Mn^{2+}	.305	1.589
F	.15			Ca	.354	.108
	100.47	97.1	96.2	Na	1.341	.303
				Σ [*M*(4)]	2.000	2.000
$-O=F$	0.06					
	100.41			Na	.246	.002
				K	.404	.017
				Σ (*A*)	.650	.019
				100 Mg/Mg+Fe+Mn	69.8	67.8
				100 Mn/Mn+Fe+Mg	13.5	28.4
				100 Na/Na+K+Ca	67.7	70.7

suggests that nearly all if not all of the iron is ferric, consistent with the 30 percent specularite in the rock. Deer, Howie, and Zussman (1963) show high Fe_2O_3 contents of eckermannite, arfvedsonite, and magnesioarfvedsonite analyses. Although Fe_2O_3 is completely absent in many members of the cummingtonite-grunerite series, and low in most (Klein, 1964), the bulk analysis and the abundant fine magnesioarfvedsonite lamellae in this cummingtonite suggest that most of the iron is ferric. This is consistent which the considerable amounts of Na and K in the

analysis which would require a large amount of the iron to be ferric for charge balance. Possibly there is also trivalent manganese.

The totals of the two electron probe analyses are 97.1 and 96.2 weight percent. The bulk analysis (Table 2, column 1) shows 3.13 weight percent H_2O and F and if similar amounts are present in the individual amphiboles their totals would be 100.4 and 99.3 respectively.

Although no quantitative analyses could be made on the lamellae because of their size, qualitative electron probe traces for MnK$\bar{\alpha}$, FeK$\bar{\alpha}$, and MgK$\bar{\alpha}$ indicate that the lamellae in cummingtonite are more Mn-poor and Fe-rich than the host, and the lamellae in magnesioarfvedsonite are more Mn-rich and Fe-poor than the host. Mg shows no such relative change because of the close similarity of MgO content of the two amphiboles. These data suggest that the lamellae in cummingtonite are magnesioarfvedsonite and vice versa. This is supported by the fact that unit cell parameters of lamellae, as determined on single crystal photographs, are very similar to those reported in Table 1 for the host amphiboles.

Possible Explanations for Orientation of Optically Observed Exsolution Lamellae

For several years we have sought an explanation for the discrepancy between optically observed orientations of exsolution lamellae and the relative orientation of lattices as observed in X-ray single crystal photographs. Three possible explanations have entered our thinking, one of which seems particularly promising at present.

(1) The exsolution lamellae are a direct "fossil" record of the β angle of the host under the *P-T* conditions where exsolution took place. This hypothesis is reasonable only for those pyroxenes and amphiboles showing smaller exsolution angles. Heating experiments on clinopyroxenes (Prewitt, Papike, and Ross, 1970; J. R. Smyth, 1970; J. V. Smith, 1969, Table 11) show that the β angle does in fact become larger at higher temperature, but only by one or two degrees. On the basis of the information now available, the hypothesis of the direct "fossil β angle" can be ruled out.

(2) Possibly on a submicroscopic scale the composition planes of the lamellae are in fact (001) and the lamellae observed under the microscope are composed of submicroscopic (001) segments lined up in some other direction. This hypothesis has yet to be tested by observations with an electron microscope. If the segments were on a unit-cell scale, this and the third hypothesis might be indistinguishable in many cases.

(3) The composition planes of the lamellae do not have the same orientation as the lattice planes along which host and lamellae appear to be oriented. Rather, the orientation of the composition planes is determined by the directions of dimensional best fit between the two lattices. This

hypothesis, recently expounded in a study of feldspars by Bollman and Nissen (1968), is referred to as the theory of optimal phase boundaries or the *O*-lattice theory. The essential features of the theory are concisely given by these authors as follows:

"We give here a brief description of the essential points of the *O*-lattice theory. In order to determine a boundary between two crystals, the structure and relative orientation of the two crystals as well as the orientation of the boundary have to be taken into account. . . . In order to determine the boundary we interpret the two crystals as *interpenetrating lattices*. Then, within the interpenetrating lattices, a boundary will be placed through points where both lattices match best. Once the boundary is chosen, only one lattice on each side is considered as real, so that now two different real crystals are separated by the boundary. The points where the two interpenetrating lattices fit best constitute the *O*-lattice."

In his discussion of pyroxene exsolution J. V. Smith (1969, p. 22) calls attention to this theory, but does not explore its consequences, although best fit considerations do enter his discussion of kink boundaries (p. 21). Although the mathematical procedure given by Bollman and Nissen was beyond our powers, the simple essence of the theory as given above made its application to pyroxenes and amphiboles by simple graphical and numerical methods an obvious step. Since the exsolution planes of interest involve lattice points in the (010) plane, analysis can be carried out in two dimensions.

Application of Optimal Phase Boundary Considerations to Pyroxenes and Amphiboles

The theory of optimal phase boundaries dictates that composition planes bounding two phases will be oriented in the directions of best dimensional fit between the two lattices. The lattice dimensions in Table 3 show that the c dimensions in various pairs do not differ greatly, and a reasonable though far from perfect fit might be expected on (100). The a dimensions, on the other hand, show much greater differences and in most cases indicate a poor fit on (001). In the five specimens for which we have lattice parameters and optical measurements of the exsolution planes, there is a striking correlation between the difference of the a dimensions of a pair of lattices and the angular difference of the measured exsolution lamellae from the β angle (Table 3). It should be kept in mind that all of the measurements of lattice parameters were made at room temperature and hence differ by an unknown amount from the parameters for the conditions under which exsolution took place. Morimoto and Tokonami (1969) have considered at length the strain effects on the lattice parameters of augite lamellae in a pigeonite host with different dimensions. Furthermore, the precision of the various measure-

TABLE 3. LATTICE PARAMETERS, CALCULATED BEST FIT PLANES, AND MEASURED ANGLES OF EXSOLUTION LAMELLAE OF PAIRS OF PYROXENES AND AMPHIBOLES

	Lattice Parameters[a]			"001" Exsolution Planes					"100" Exsolution Planes			
					Calculated Best Fit					Calculated Best Fit		
	a	c	β	a-a	w	Diff.[b] from β	Angle	Measured[c] Exsolution Angle	c-c	w	Angle[b]	Measured[c] Exsolution Angle
1. Diopside	9.748	5.251	105°40′	.142	1.15	21°46′	127°26′		.076	4.00	21°39′ acu	
Clinoenstatite	9.606	5.175	108°20′			21°08′	129°28′				21°01′ acu	
2. Magnesioarfvedsonite	10.018	5.295	106°49′	.111	1.49	17°07′	123°56′	123°	−.019	−16.47	6°29′ obt	6° obt
Manganoan Cummingtonite	9.907	5.314	108°45′			17°00′	125°45′	125°			6°25′ obt	6° obt
3. Hedenbergite	9.845	5.248	104°45′	.136	2.15	12°44′	117°29′		.020	27.18	3°45′ acu	
Clinoferrosilite	9.7085	5.2284	108°26′			12°26′	120°46′				3°38′ acu	
4. Augite host	9.776	5.252	105°55′	.081	2.60	10°39′	116°34′	116°	(.016)	(24.98)	(4°01′ acu)	6° acu
											54′ acu	
Pigeonite lamellae "001"	9.695	5.236	108°33′			10°28′	119°01′		.004	111.26	(3°56′ acu)	
Pigeonite lamellae "100"	9.694	5.248	108°50′								54′ acu	
5. Manganoan tremolite host	9.889	5.273	106°20′	.063	3.93	7°09′	113°29′	114°	−.007	−67.34	1°33′ obt	5° obt
Manganoan P-Cummingtonite lamellae "001"	9.82$_8$	5.28	109°14′			7°03′	116°17′				1°31′ obt	
6. Augite lamellae "001"	9.75	5.26	105°48′	.06	4.00	7°23′	112°56′		.03	14.83	6°38′ acu	
Pigeonite host	9.69	5.23	108°48′			7°16′	115°47′				6°29′ acu	
7. Hornblende lamellae "001"	9.90$_1$	5.33	106°31′	.027	9.81	2°58′	109°29′	110°?	.02	24.60	4°03′ acu	? acu
Cummingtonite host	9.87$_4$	5.31	109°39′			2°54′	112°33′	112°			3°58′ acu	2° acu
8. Hornblende host	9.87$_1$	5.32	106°45′	−.009	−29.65	−1°00′	105°45′	105°			4°24′ acu	4° acu
									.02	22.60	(2°03′ acu)	
Cummingtonite lamellae "100"	9.87$_0$	5.30	109°35′								4°19′ acu	
Cummingtonite host	9.88$_0$	5.31	109°49′			−59′	108°50′	108°	(.01)	(49.31)	(2°00′ acu)	2° acu

[a] Pyroxene C-cell, amphibole I-cell, or equivalent primitive cells.
[b] Relative rotation of the lattices is equivalent to the difference between these two angles.
[c] Optically measured angles accurate to ±1°.
1. Hypothetically matched synthetic pure phases, Smith, 1969, Table 11.
2. Labrador, this paper, Table 1.
3. Hypothetically matched synthetic pure phases, Lindsley, Munoz, and Finger, 1969; Smith, 1969, Table 1.
4. Hudson Highlands, Jaffe and Jaffe, 1971; this paper, Table 5.
5. Northwest Adirondacks, Ross, Papike, and Shaw, 1969, Table 2, specimen G-24.
6. Ferrogabbro, Skaergaard Intrusion, Morimoto and Tokonami, 1969.
7. Southwestern New Hampshire, Robinson and Jaffe, 1969; Ross, Papike, and Shaw, 1969, Table 6, specimen 7A8BX, crystal 2.
8. Central Massachusetts, Robinson and Jaffe, 1969; Ross, Papike, and Shaw, 1969, Table 6, specimen 7E8BX, crystals 2, 1.

ments is variable. All of these uncertainties, however, justify our use of simple graphical and numerical procedures to locate the plane of best fit between lattices. When more abundant, more precise, measurements are available, especially at high temperatures and pressures, use of more sophisticated computer techniques will obviously be justified.

We first resorted to a graphical method, comparing the fit between two lattices laid out on tracing paper. Since the true differences between the cell dimensions are small, high precision must be maintained, the scale of the paper unit-cells must be very large ($a \sim 13$ cm in our attempt), and hence only a small number of cells can be drawn up on a manageable sheet of paper. In the case of the natural magnesioarfvedsonite-manganoan cummingtonite pair with the poorest fit of the a dimensions, the graphical procedure proved reasonably satisfactory (Fig. 4). For all other natural examples simple numerical procedures proved more suitable.

The simplest numerical procedure consists of listing the coordinates of a series of lattice points in rows parallel to the (001) plane (Table 4). In the first row the points of the two lattices are parallel and in the same vertical position, and the two lattices are superimposed at the origin at coordinates 0,0. The coordinates of the remaining lattice points in the first row are multiples of the a dimension. The second row of each lattice is offset upward from the first by the amount $c \sin \beta$ and lattice points in

TABLE 4. COORDINATES OF LATTICE POINTS IN (010) FOR MAGNESIOARFVEDSONITE (TOP) AND MANGANOAN CUMMINGTONITE (BOTTOM) THAT SHARE A COMMON (001) PLANE

Figures in first significant column in each row are given to three decimal places to avoid multiplication of rounding error in subsequent columns.

	z-coordinates								
	20.274	6.127	16.15	26.17	36.18	46.20	56.22	**66.23**	76.27
	20.127	6.833	16.74	26.64	36.55	46.46	56.37	**66.28**	76.18
	15.206	4.596	14.62	24.64	34.65	44.67	**54.69**	64.71	74.73
	15.095	5.124	15.03	24.93	34.84	44.75	**54.66**	64.56	74.47
	10.138	3.064	13.08	23.10	**33.11**	43.13	53.15	63.17	73.19
	10.063	3.416	13.33	23.23	**33.14**	43.05	52.96	62.86	72.77
	5.069	1.532	11.55	**21.57**	31.59	41.60	51.62	61.64	71.66
	5.031	1.708	11.62	**21.52**	31.43	41.34	51.24	61.15	71.06
Mg-arfv.	0	0	10.018	20.04	30.05	40.07	50.09	60.11	70.13
Mn-cumm.	0	0	9.907	19.81	29.72	39.63	49.54	59.44	69.35
Origin		x-coordinates							

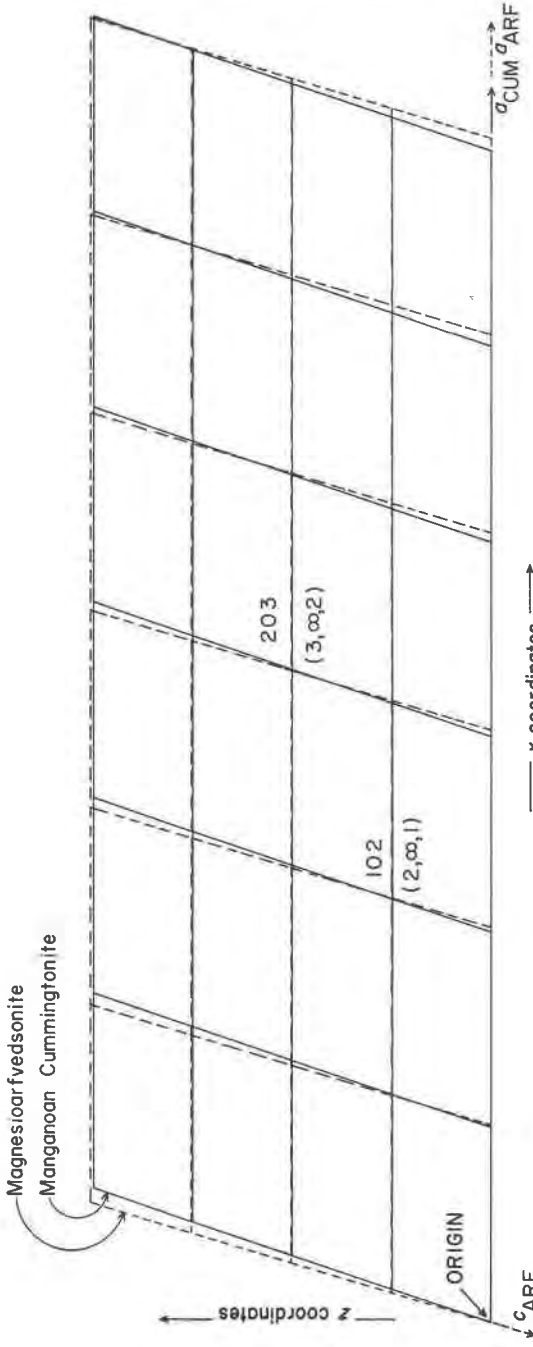

FIG. 4. Lattices of magnesioarfvedsonite and manganoan cummingtonite, both space group $I2/m$, viewed in the (010) plane. The lattices share a common orientation of their (001) planes. Lattice planes (102) [intercepts 2, ∞, 1] and (203) [intercepts 3, ∞, 2] are closest to the irrational plane of dimensional best fit between the lattices. Dimensional fit can be perfected by relative rotation of magnesioarfvedsonite lattice by 7°clockwise.

the second row are moved along the row by an amount $c|\cos\beta|$. The x coordinate of any lattice point in the second row is thus equal to the x coordinate of the first point in the row ($c|\cos\beta|$) plus the number of units of the a dimension along the row (na); thus:

$$x = c|\cos\beta| + na \tag{1}$$

The third row is offset and moved from the second row in the same manner and so on.

In each row it can be seen that there is a pair of x coordinates that represents the closest fit in that direction. Closest fit locations can be made more obvious to rapid inspection by placing an overlay on Table 4 and preparing a table of differences between the x coordinates. The orientation of the plane of best fit can be approximately located by finding the pair of lattice points with the best fit in their x coordinates in the second row. In practice it would be coincidence for the fit between the two lattices to be good at integral numbers of unit cells, because the true best fit planes are irrational. Thus for purposes of finding the angle of the best fit plane the number of a units need not be integral and a variable, w, may be substituted for n. The location of best fit in the second row is the point where the x coordinates are equal. Thus the two equations for the x coordinates for the two lattices (using augite and pigeonite as examples) may be solved for w.

$$c_{AUG}|\cos\beta_{AUG}| + wa_{AUG} = c_{PIG}|\cos\beta_{PIG}| + wa_{PIG}, \tag{2}$$

and

$$w = \frac{c_{PIG}|\cos\beta_{PIG}| - c_{AUG}|\cos\beta_{AUG}|}{a_{AUG} - a_{PIG}} \tag{3}$$

If w is close to integral, it may be used to give the Miller indices of the rational plane closest to the irrational best fit plane. If w is not close to integral, it may be multiplied by successive integers until a product that is nearly integral is found. However, because the true composition plane is generally irrational, we favor the direct use of w to solve for the angle of the plane. The angle of the best fit plane to (001) is the angle whose tangent is the z coordinate of the second row divided by the x coordinate of the best fit location in the second row. The angle from (001) is then added to β to give the exsolution angle. Thus; the

predicted "001" exsolution angle of augite is equal to

$$\beta_{AUG} + \arctan\frac{c_{AUG}\sin\beta_{AUG}}{c_{AUG}|\cos\beta_{AUG}| + wa_{AUG}}. \tag{4}$$

It can be seen by inspecting the column in Table 4 headed "z-coordi-

nates" that with each additional row the fit in the vertical direction deteriorates by an amount related to the difference between the values of $c \sin \beta$ for the two lattices. Thus in row 2 of Table 4 the best fit has x coordinates 21.57, 21.52—the horizontal misfit is .05, the vertical misfit is .04. In row 3 the best horizontal fit has coordinates 33.11, 33.14—the horizontal misfit is .03, the vertical misfit is .08. One thing that can be done to improve the vertical fit is to rotate the magnesioarfvedsonite lattice slightly in a clockwise direction until the vertical position of one of its best fit lattice points is the same as that of the corresponding cummingtonite lattice point. Thus, on rotation of the magnesioarfvedsonite lattice by 7′ about the b axis, so that its c axis moves toward the c axis of cummingtonite, the magnesioarfvedsonite point with z and x coordinates of 5.069, 21.57 becomes 5.031, 21.58, and point 20.274, 66.23 becomes 20.127, 66.27. A similar rotation of 9′ causes magnesioarfvedsonite point 10.138, 33.11 to become 10.063, 33.13. The amount of relative rotation required to achieve a vertical fit in a given case is related to the relative values of $c \sin \beta$ and the a misfit for the two lattices. In all of the natural pairs we have examined so far $c \sin \beta$ for the mineral (AUG) with the smaller β angle is greater than $c \sin \beta$ for the mineral (PIG) with the larger β angle ($c \sin \beta_{AUG} > c \sin \beta_{PIG}$), even in those cases where the c dimensions show the opposite relationship ($c_{AUG} < c_{PIG}$). If the special circumstance existed where the values for $c \sin \beta$ were equal, the vertical fit would be already established and no rotation would be required. In this special circumstance it can be shown geometrically that the two lattices share *two* common planes of orientation, the irrational plane of dimensional best fit, and (001) which is a plane of poor dimensional fit.

If the dimensional fit can be improved by relative clockwise rotation as shown, why is it that the X-ray single crystal photographs show the lattices with their (001) planes essentially parallel? We suggest that their (001) planes are *not exactly* parallel, but that, because of the very great similarity of the lattices involved, the amount of rotation required to achieve nearly perfect dimensional fit along the irrational contact plane is slight. In the natural cases we have examined here the required rotation is less than 12′ and might not be easily detectable on single crystal X-ray precision photographs. In the artificial matching of pure diopside and pure clinoenstatite (Table 3) the required rotation is 42′ and this increases predicted exsolution angles by about 4°. Morimoto and Tokonami (1969, Fig. 3) did show that (001) of augite lamellae is rotated about 54′ (0.9°) counterclockwise from (001) of a pigeonite host, the opposite rotation from that described above. A possible interpretation of this counterclockwise rotation is given at the end of this paper.

To summarize, the X-ray single crystal photographs given the relative orientation of the *lattices* of the host and lamellar phases. In most crystals thus far examined by X-ray precession photography the exsolution lamellae have their (001) and (100) lattice planes oriented, within an accuracy of a few minutes arc parallel to the (001) or (100) lattice planes of the host. In a few crystals we have studied but not reported here misorientation is as much as 30′. The optical measurements give the angular orientation of the composition planes of the exsolution lamellae with respect to the lattice of the host. Generally the angular orientation of these composition planes deviates significantly from the (001) or (100) of the host lattice planes. The composition plane is the plane of best fit. The lamellae are parallel to this plane because it is the plane of nucleation of lamellar crystal growth. Generally a small rotation of the host and lamellae lattices from an ideal (001) or (100) orientation is necessary to cause a more perfect match within the composition plane. These small rotations are difficult to detect in X-ray photographs.

In order to take into account possible rotation of the lattices to achieve best dimensional fit, we have derived a trigonometric approximation to rotation about the origin. In solving for w (equations 2 and 3) the x coordinate of an augite best fit position is increased by an amount x_1 as a result of clockwise rotation. x_1 is the base of a small right triangle that has as its hypotenuse the chord of the arc of rotation, and as its height (z_1) the vertical displacement between the augite and pigeonite rows ($c_{AUG} \sin \beta_{AUG} - c_{PIG} \sin \beta_{PIG}$). Since the amount of rotation is small and the curvature is slight, the angle (θ) and slope ($\tan \theta$) of the chord of the arc of rotation may be approximated from the previously determined coordinates (z, x) of the unrotated augite best fit point, thus: $\tan \theta = x/z$. Since $\tan \theta$ is also equal to z_1/x_1 in the small triangle, it follows that:

$$x_1 = \frac{z_1}{\tan \theta} = \frac{z_1}{x/z} = \frac{(c_{AUG} \sin \beta_{AUG} - c_{PIG} \sin \beta_{PIG})}{x/z} \tag{5}$$

Applying this to equation 3) we get:

$$w = \frac{c_{PIG} \left| \cos \beta_{PIG} \right| - c_{AUG} \left| \cos \beta_{AUG} \right| + \dfrac{(c_{AUG} \sin \beta_{AUG} - c_{PIG} \sin \beta_{PIG})}{x/z}}{a_{AUG} - a_{PIG}} \tag{6}$$

In the case where the a dimension of augite is less than that of pigeonite ($a_{AUG} < a_{PIG}$) the denominator of equation 6) becomes negative, w becomes negative, the x coordinate of the best fit position becomes negative, and the best fit plane lies in the obtuse angle β at an angle to the c-axis

less than β. The relationships between the relative values of the a dimensions and the orientation of exsolution planes are illustrated at the top of Figure 5, including the special case where the a dimensions are equal and w becomes infinite.

It is obvious that if the relative a dimensions control the orientation of "001" exsolution lamellae, so the relative c dimensions must control the orientation of "100" lamellae. The same equations, 3), 4), and 6), can be used to evaluate the effect of c misfits, except that where a appears in the original versions it must be replaced by c and vice versa. In the case where c of augite is greater than c of pigeonite ($c_{AUG} > c_{PIG}$), w will be positive, the x coordinate of the best fit position (now measured parallel to the c direction) will be positive, and the exsolution plane will lie in the acute angle β. Conversely, when c of augite is less than c of pigeonite ($c_{AUG} < c_{PIG}$), w will be negative, and the exsolution plane will lie in the obtuse angle β. These relationships, including the special case where the c dimensions are equal, are illustrated in the lower half of Figure 5.

As stated above, the amount of lattice rotation required to achieve best fit in the case of an a misfit is a function of the relative values of $c_{AUG} \sin \beta_{AUG}$ and $c_{PIG} \sin \beta_{PIG}$. For a c misfit, conversely, rotation should be a function of the relative values of $a_{AUG} \sin \beta_{AUG}$ and $a_{PIG} \sin \beta_{PIG}$. Thus, for each of the six possibilities illustrated in Figure 5, there are three possibilities for relative lattice rotation or lack of rotation as illustrated in Figure 6. Eight of these are general cases requiring lattice rotation, and ten are special cases that require no rotation. In natural clinopyroxenes and clinoamphiboles the cases (Fig. 6) in the first row of each group of six (1-1, 2-1, 3-1, 4-1, 5-1, 6-1) are most probable. The examples in the second and third rows require very large differences in the a or c dimensions and are not expected to be so common. However, these should not be ruled out, particularly if there are pyroxene pairs with small differences in their β angles. In all of our considerations, we have, of course, avoided possible misfits of the b dimensions which would require evaluation in three dimensions. Generally (M. Ross, unpublished data) the b dimensions of host and lamellae are nearly identical.

Calculated Best Fit Planes and Measured Angles of Exsolution Lamellae

Calculated best fit planes and measured angles of "001" and "100" exsolution lamellae for natural clinopyroxenes and clinoamphiboles are listed in Table 3 together with hypothetical pairings of two sets of synthetic pyroxene end members. Accurate calculation of best fit planes

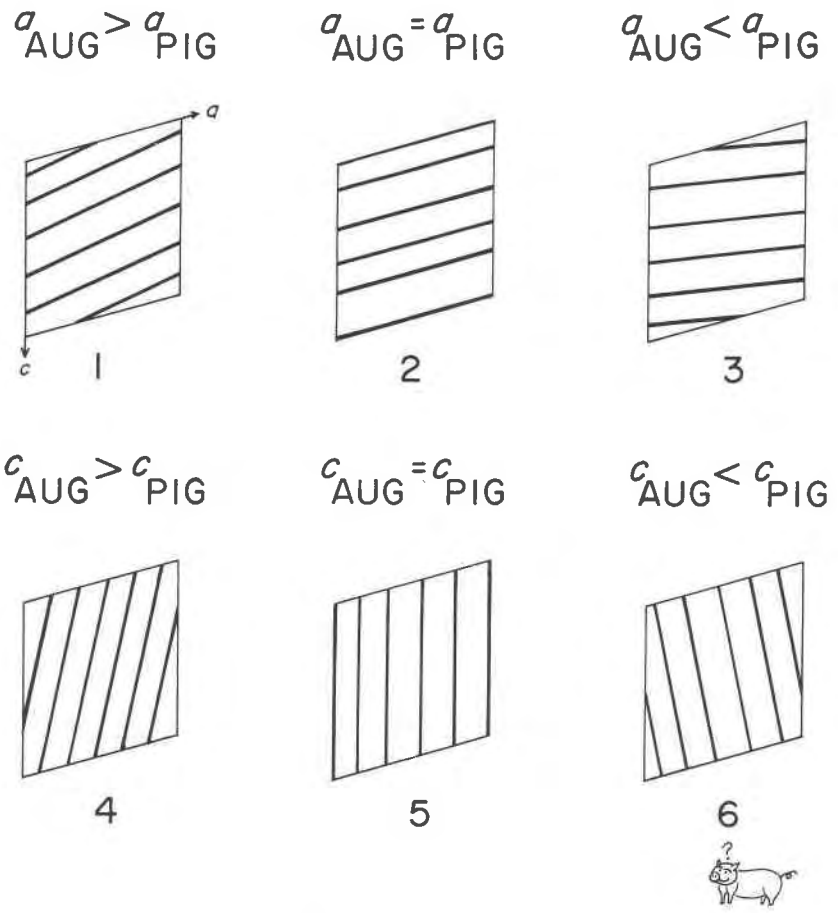

FIG. 5. Relationship between relative a and c dimensions and the orientation of exsolution lamellae in clinopyroxenes and clinoamphiboles. Rhombs represent schematic crystals bounded by (001) and (100) planes. Apologies to George Orwell.

requires lattice parameters given to three decimal places. Such measurements are usually obtained by refinement of powder data on separated host phases. However, real best fit planes are determined by host-lamellae relations, and lattice parameters of lamellae are easily obtained only in single crystal photographs. We have given the calculated best fit planes to the nearest minute with the full realization that for lattice parameters based on single crystal data, particularly in the case of "100" planes, the calculated planes may be in error by as much as 2°.

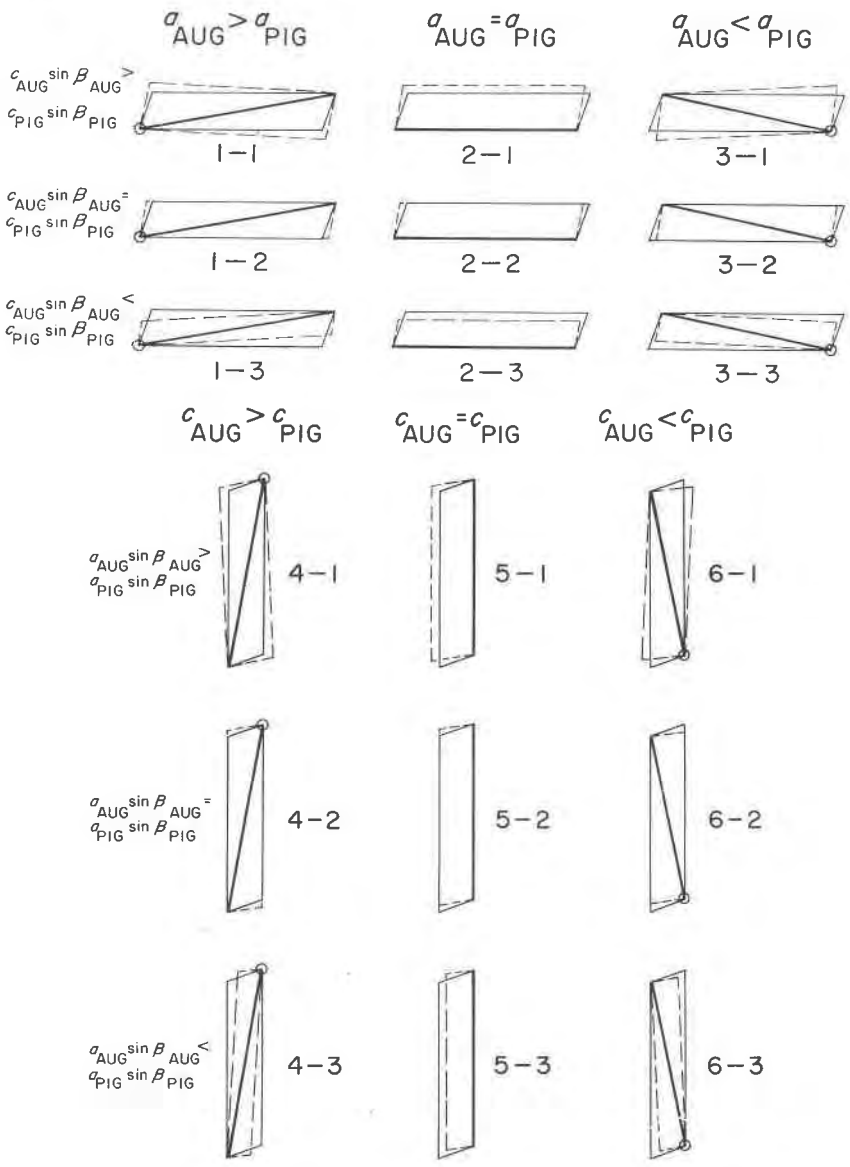

FIG. 6. Relationships between relative values of a and c dimensions, relative values of $c \sin\beta$ and $a \sin\beta$, orientation of exsolution lamellae, and kind of lattice rotation required to achieve best dimensional fit between lattices. Position of origin circled. In diagrams 1-1 to 1-3 and 3-1 to 3-3 each parallelogram (shown schematically) has a height equivalent to $c \sin\beta$ and a length equivalent to $c|\cos\beta| + wa$. In diagrams 2-1 to 2-3 fit is perfect on (001) and length of parallelograms is meaningless. Dashed lines represent the phase with

Measurements of the angles of exsolution lamellae have been made in thin section or in grains under oil immersion. Angles between "001" and "100" lamellae can be quite accurately measured in thin section on the universal stage, but the location of the *c*-crystallographic axis on the basis of traces of $\{110\}$ cleavage is virtually impossible and very fine "100" lamellae are very difficult to see. In oils the prismatic cleavages parallel to *c* are much easier to identify and extremely fine "100" lamellae can be seen if an oil is chosen with an index of refraction close to that of the mineral. Correct exsolution angles can be observed when a prismatic grain is oriented so that the extinction angle $Z \wedge c$ is at a maximum. In one case (Table 3, no. 7), where the "100" exsolution lamellae make a small angle with the $\{110\}$ cleavage traces and are very abundant, they influence the way the mineral breaks and make accurate location of the *c* axis nearly impossible. We think the stated limits of accuracy of $\pm 1°$ are very realistic for most of these measurements.

Optically observed angles of exsolution lamellae should be closely related to the relative lattice parameters under the conditions where exsolution began. Calculated best fit planes should reflect mean lattice parameters under the conditions of X-ray measurement. The very close agreement between calculated and observed "001" planes in Table 3 suggests that for these samples there has not been much change in relative cell parameters, particularly the *a* misfit, since exsolution was initiated. This observation should not be surprising because four of the specimens are amphiboles with a thermal history below about 650°C and the fifth is a metamorphic pyroxene probably formed below 800°C. At the same time the close agreement seems to be a remarkable confirmation of the optimal phase boundary theory. Agreement of calculated and measured "100" planes is poorer, possibly because of inaccuracies in the measurements of *c* or difficulties in the optical measurements in specimens 5, 7, and 8. In the case of the pyroxene the difference could be due to a change of the *c* dimensions since the beginning of exsolution and this possibility will be explored below.

All four of the general cases in Figure 5 (1, 3, 4, and 6) are represented by the specimens in Table 3. Of the *a* misfits, case 1 is the common one, and we have only one example of case 3 (No. 8) in which the hornblende

---

the smaller β angle (AUG) and solid lines represent the phase with the larger β angle (PIG). In diagrams 4-1 to 4-3 and 6-1 to 6-3 the height of the parallelograms is equivalent to $a|\cos\beta|+wc$, and the width is equivalent to a $\sin\beta$. In diagrams 5-1 to 5-3 fit is perfect on (100) and height of parallelograms is meaningless.

has a very high Al content. Of the c misfits there are four natural examples of case 4 and two of case 6. Three out of the four possible combinations of a and c misfits are represented in Table 3. Nos. 4, 6, and 7 are a combination of case 1 and case 4. We have observed numerous other metamorphic pyroxenes from the Adirondacks with this combination, and predictions from the pairs diopside-clinoenstatite (No. 1) and hedenbergite-clinoferrosilite (No. 3) suggest this may be the usual combination for compositions in the clinopyroxene quadrilateral formed at intermediate to low temperature. Nos. 2 and 5 are a combination of case 1 and case 6. These specimens are both manganese-rich and the possibility exists that they mimic features that would appear in more normal Mg- and Fe-rich specimens only at high temperature (see below). No. 8 is a combination of case 3 and case 4, and we have not yet found a combination of case 3 and case 6.

Petrologic Significance of Exsolution Angles

We have pointed out above that the exsolution angle should be controlled by the lattice parameters under the conditions of exsolution, which were probably somewhat different than those measured at room temperature. This may be referred to as the *thermal expansion effect.* A different temperature-dependent aspect turns up in examination of the pyroxene data in Table 3. The pair diopside-clinoenstatite (No. 1) is matched in a completely artificial way, because pure diopside and pure clinoenstatite would not be found together in nature. The diopside would have some clinoenstatite in solid solution and vice-versa. Thus, not only are the pure diopside and pure clinoenstatite far apart compositionally as compared to a natural clinopyroxene pair, but their cell parameters, particularly their a dimensions, show larger differences than natural pairs such as augite and pigeonite from the Skaergaard intrusion (Table 3, No. 6). The larger difference between the a dimensions for the artificial pair result in larger predicted angles for "001" exsolution planes, larger in fact than any which have yet been observed in nature. The same is true of the difference between the c dimensions and the "100" exsolution planes. In the cases of natural igneous pyroxene pairs, formed under high temperature with a relatively narrowed miscibility gap, the differences in the a dimensions would be small and hence the exsolution angles could be fairly close to β. This could be the reason why anomalous angles of exsolution lamellae have not been reported from the thoroughly studied pyroxenes of the layered mafic intrusions (Poldervaart and Hess, 1951; Brown, 1957), although we suspect no one has thoroughly looked. On the other hand, under conditions of metamorphism at lower temperature,

where pyroxene and amphibole miscibility gaps would be wider, differences in a dimensions would generally be larger, and exsolution angles might be expected to be larger, as in the specimen from the Hudson Highlands (No. 4, Table 3). This temperature dependent effect of the solvus on the angle of "001" exsolution lamellae may be referred to as the *solvus effect* and should increase the angle of exsolution as temperature falls. It is less easy to generalize concerning the *thermal expansion effect* on the angle of "001" exsolution. Heating experiments (see above) have shown that the β angle does increase with rising temperature, but the effect on the difference in a dimensions, which may be more important, is not clear, except in the case of the hypothetically matched pair diopside-clinoenstatite (Smith, 1969) at 1000–1100°C where the a dimension of clinoenstatite is larger than that of diopside. By analogy with this example, the *solvus* and *thermal expansion* effects would both seem to reduce the difference in a dimensions.

Combined X-ray, electron probe, and microscopic investigation of the solvus effect could reveal significant details of thermal history. Kuno and Hess (1953) and Brown (1960) have given preliminary diagrams showing the variation of lattice parameters in the clinopyroxene quadrilateral diopside-hedenbergite-clinoenstatite-clinoferrosilite. Application of electron probe analyses of host and lamellae to greatly refined versions of these diagrams, possibly based on high temperature and pressure cell parameters, should allow prediction of cell parameters of host and lamellae, and hence the exsolution angle. Boyd and Brown (1969) have emphasized the continued re-equilibration which has taken place between host and lamellae long after the initiation of exsolution. The dimensions predicted by the method described above, or measured directly, might give a predicted exsolution angle larger (and indicative of lower temperature) than the angle actually observed. The observed exsolution angle might be used to predict the cell dimensions and, in turn, the compositions of the host and lamellae at the time exsolution was initiated. None of these measurements will be easy and progress will be slow.

The possibilities for the solvus effect are illustrated by a specimen of augite from the Duluth Gabbro (Fig. 7, Table 5). This augite is inhomogeneous, showing pyroxene exsolution lamellae, blebs of ulvospinel and ilmenite, and evidence on the edges of the grains of reaction with surrounding minerals. In some areas, as in Figure 7, there are three sets of pyroxene exsolution lamellae, two containing ulvospinel blebs and one which is free of oxides. An X-ray single crystal photograph (Table 5) of a grain selected at random shows only two lattice orientations of pyrox-

ene exsolution rather than three as might be expected from inspection of Figure 7. The coarsest lamellae in Figure 7, with the larger ulvospinel blebs, are hypersthene oriented parallel to (100) of the augite host. The second set of lamellae with the small oxide blebs is pigeonite with its (001) lattice planes oriented parallel to (001) of the augite host. These lamellae lie at an angle of 108–109° to the *c*-crystallographic axis. The third set of lamellae, which is free of oxides and apparently later than the others, is also pigeonite with its (001) lattice planes oriented parallel to (001) of the host. These lamellae make an angle of 111–115° with the *c*-crystalographic axis. The lattice parameters for augite host and pigeonite lamellae in Table 5, which represent the mean for the whole grain examined by X-ray, yield a calculated best fit plane for "001" lamellae of 114°2′ which is close to the upper limit of the range of measurements for the third set of lamellae.

Our interpretation of Figure 7 in terms of the solvus effect is as follows. Subcalcic augite crystallized from the gabbroic magma. Cooling caused the initial exsolution of pigeonite "001" lamellae and, at the same time, hypersthene with its (100) lattice planes oriented parallel to (100) of the lattice of the augite host. At this time the bulk composition of the augite was appropriate to exsolve a pigeonite with a composition and cell dimensions that would give a 108° best fit plane with the augite host. On further cooling the augite was further depleted in the hypersthene component by growth of pigeonite and hypersthene lamellae, and the pigeonite and hypersthene lamellae were depleted in augite component which diffused into the host. The unmixing of pigeonite and hypersthene during this stage was apparently accompanied by exsolution of ulvospinel within both sets of lamellae. As exsolution proceeded the solvus effect on the relative cell dimensions caused the dimensional fit along the previously selected 108° plane to become progressively poorer. In some parts of the crystal the dimensional misfit eventually became so large that it became energetically more suitable to nucleate new exsolution planes rather than to continue adding material to those of the old orientation. The range from 111° to 115° of the new exsolution lamellae suggests this critical state may have been reached at slightly different augite compositions and perhaps slightly different temperatures in different parts of the crystal. The 114° angle of the best fit plane calculated from cell parameters measured at room temperature suggests that the mean lattice parameters have not changed substantially since this last phase of exsolution. Just inside some margins of augite grains, where the augite was apparently depleted early in hypersthene component by reactions with surrounding minerals or liquid, it contains none of the early lamellae. This augite did

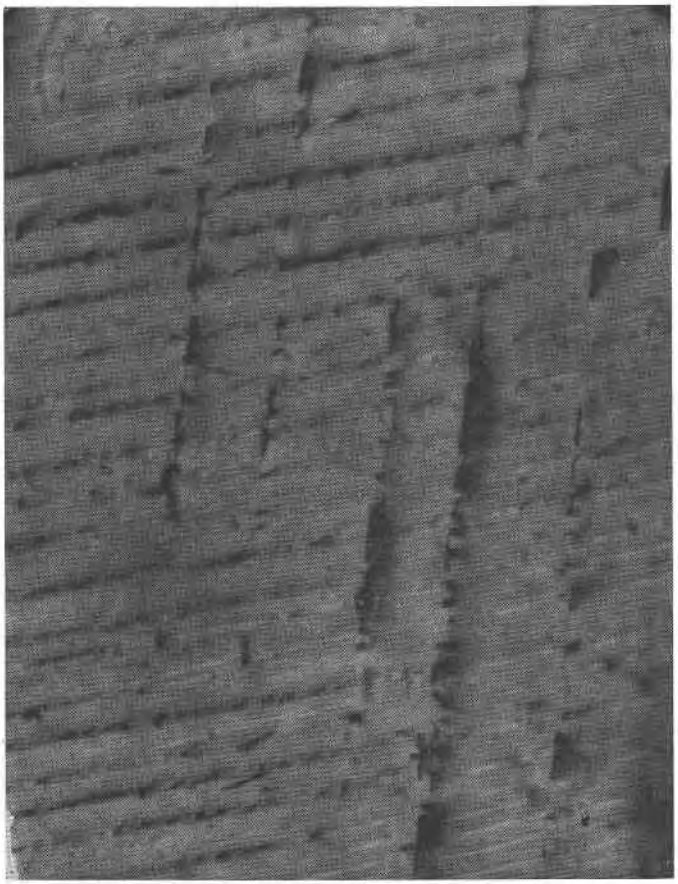

FIG. 7. Photomicrograph of augite from the Duluth Gabbro, Minnesota. View of thin section cut normal to (010) showing three sets of exsolution lamellae. The coarsest lamellae, containing oxide blebs, are hypersthene oriented parallel to (100) of the host. The second set of lamellae with oxide blebs is pigeonite and lies at an angle of 108° to the *c*-crystallographic axis of the augite host. The third set of lamellae, which is free of oxide blebs, is also pigeonite and makes an angle of 111° to 115° with the *c*-crystallographic axis. Width of view is 0.16 mm.

not again reach saturation until the very last stages, when compositions and cell dimensions were appropriate for exsolution of lamellae at an angle of about 115°.

The exsolution lamellae in a hornblende-cummingtonite specimen (No. 8, Table 3) demonstrate that generalizations concerning the solvus effect must be made with caution. This specimen is from the kyanite zone of regional metamorphism and probably formed at a lower temperature

TABLE 5. CRYSTALLOGRAPHIC DATA FOR TWO AUGITES AND EXSOLVED LAMELLAE

	Space Group	*a*	*b*	*c*	*β*
Hudson Highlands (Jaffe and Jaffe, 1971)					
Augite host (90%)	$C2/c$	9.77_6	8.89_0	5.25_2	105°55′
Pigeonite lamellae on "001" (2%)	$P2_1c$	9.69_5	8.89_0	5.23_6	108°33′
Pigeonite lamellae on "100" (5%)	$P2_1c$	9.69_4	8.89_0	5.24_8	108°50′
Hypersthene lamellae on "100" (3%)	*Pbca*	18.35	8.89_0	5.24_8	
Duluth Gabbro (Ross, unpublished, specimen Dl-Gb-1)					
Augite host (77%)	$C2/c$	9.69_7	8.90_5	5.23_0	106°0′
Pigeonite lamellae on "001" (10%)	$P2_1c$	9.65_6	8.91_7	5.19_4	108°55′
Hypersthene lamellae on "100" (10%)	*Pbca*	18.22	8.88	5.21	
Ilmenite (3%)	$R3$	5.07		13.99	

"001" Exsolution planes in Duluth Gabbro Augite

			Calculated Best Fit Plane		Measured Exsolution Angles
	a-a	*w*	Diff. from *β*	Angle	
Augite host	.041	3.49	8°2′	114°2′	108–109°, 111–115°
Pigeonite lamellae "001"			(7°54′)	(116°49′)	

than most of the other specimens we have examined. The "001" exsolution lamellae in both hosts lie at an angle *less than* the *β* angle. In agreement with this the hornblende has an *a* dimension slightly *less* than the *a* dimension of the cummingtonite. The unusually small *a* dimension of hornblende in this case appears to be due to a very high content of octahedral and tetrahedral Al.

The poor agreement for the Hudson Highlands augite (No. 4, Table 3) between the calculated best fit plane and the measured "100" exsolution lamellae led us to consider the possibility that the difference in *c* dimensions of augite and pigeonite was considerably larger under conditions of exsolution that at present. Consideration of the heating experiments shows that, at one atmosphere, the *c* of clinoenstatite increases more than the *c* of diopside, so that the difference in *c* dimensions decreases and by 1000–1100°C, above the low clinoenstatite-high clinoenstatite inversion temperature, is negative. Since increased temperature alone has the opposite effect of the one required, it is possible that increased pressure would have the required effect of shortening the *c* axis of pigeonite more

than the c axis of augite. At present there are no good high pressure measurements on the cell parameters of pyroxenes. One can imagine, for a given composition pair, a $P-T$ diagram (Fig. 8) separated into two regions by a univariant line of positive slope where $c_{AUG} = c_{PIG}$. The region where $c_{AUG} < c_{PIG}$ would lie on the high temperature, low pressure side of the boundary. The region where $c_{AUG} > c_{PIG}$, in which the Hudson Highlands and Adirondack specimens formed, would lie on the low temperature, high pressure side. This does not imply that these specimens formed at pressures more than 1–2 kb, because the slope and position of the boundary is unknown. Obviously the hypothetical boundary line would have a different position and slope for different composition pairs. For example, the pair magnesioarfvedsonite-manganoan cummingtonite (No. 2, Table 3) formed at moderate metamorphic temperatures but in the region where $c_{AUG} < c_{PIG}$. Apparently for this composition pair the univariant line $c_{AUG} = c_{PIG}$ would have a low or negative intercept on the temperature axis at zero pressure. Addition to Figure 8 of a second univariant line where $a_{AUG} = a_{PIG}$, related both to solvus and thermal expansion effects, produces an array of possible relations between pressure, temperature, and exsolution angles. It should be emphasized again that the lamellae angles observed should be related to the conditions where the lamellae nucleated, and that angular relationships should not change continuously as conditions change over the grid. In this sense the lamellae as observed are a "fossil" from a previously existing condition.

Another explanation for the discrepancies observed in the Hudson Highlands augite has to do with changes in composition and c dimensions following exsolution. Consider a given composition tie line at the beginning of exsolution near the center of the pyroxene quadrilateral. The coexisting augite and pigeonite "100" lamellae will have a difference in c dimensions appropriate to the conditions and composition at that moment. With cooling, however, there will tend to be Fe/Mg fractionation between augite host and pigeonite lamellae such that pigeonite will become relatively Fe-enriched. Examination of the c dimensions of the clinoenstatite and clinoferrosilite corners of the pyroxene quadrilateral (Table 3, Nos. 1 and 3) shows that increased Fe content will increase the c dimension of pigeonite, decrease the difference between the c dimensions of augite and pigeonite, and hence decrease the angle of the best fit plane between the lattices. Since augite is the host and is a relatively abundant reservoir of Fe, its bulk Fe content should not change appreciably. In the reverse case, where pigeonite is the host and the "100" lamellae are augite, the augite would become enriched in Mg and the pigeonite would remain nearly the same. Because c dimensions along the

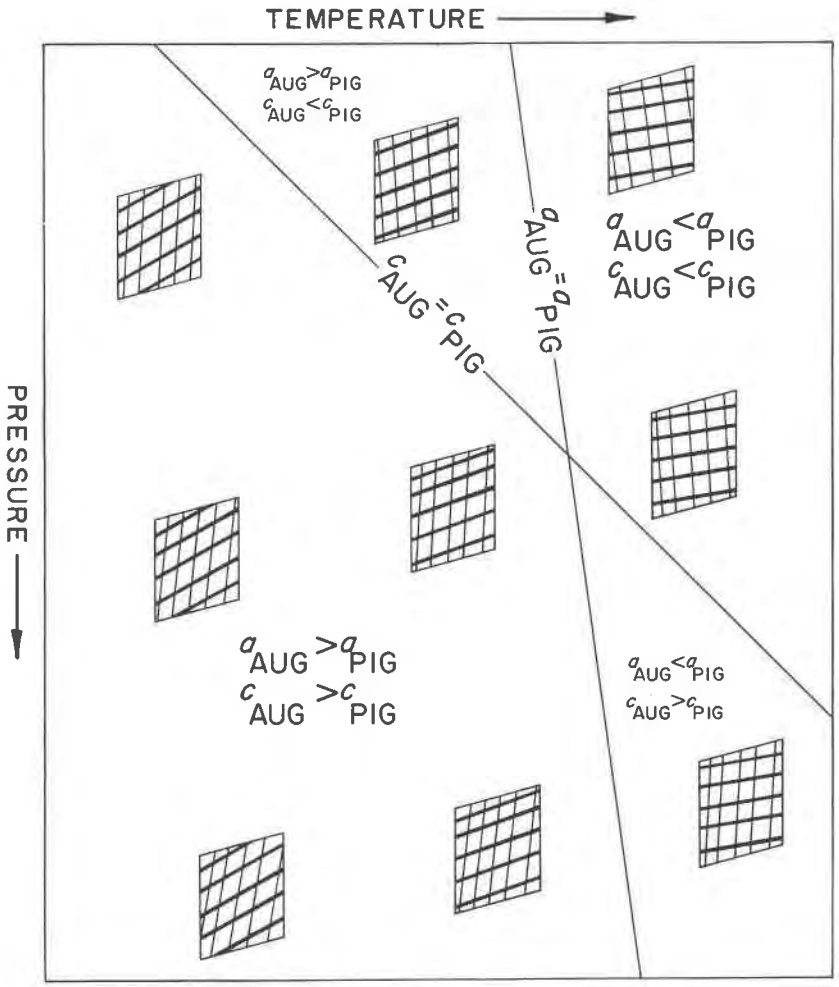

FIG. 8. Pressure-temperature diagram for a hypothetical pyroxene composition pair, showing possible effects of pressure and temperature on relative a and c dimensions, and hence on the angles at which exsolution lamellae will nucleate. Three out of the four topological arrangements of lamellae are represented by specimens listed in Table 3. The pressure and temperature scales, both absolute and relative, are completely unknown, and would be expected to differ greatly for different bulk compositions.

diopside-hedenbergite join are nearly the same, the c of augite lamellae would not change as a result of the composition effect, the difference in c dimensions would not change, and the angle of the best fit plane would not decrease. This hypothesis could be tested if a sample could be found

that had a sufficiently long thermal history and contained both augite and pigeonite hosts, both with "100" lamellae.

One puzzling feature of the Skaergaard pigeonite with "001" augite lamellae reported by Morimoto and Tokonami (1969) is the angular relationship of the lattices shown in their single crystal photograph. Using their room temperature cell parameters (Table 3, No. 6) we can show that the augite lattice should be rotated 7′ in a *clockwise* direction to achieve best fit with the pigeonite host. Their single crystal photograph and text show, however, that the (001) plane of the augite lattice is rotated 54′ (0.9°) in a *counterclockwise* direction from (001) of the host. Is it possible that the lattice orientation on the single crystal photograph is a reflection of the relative lattice orientation, dimensions, and best fit position at the time exsolution commenced? Figure 6 shows that there are two cases, 1–3 and 3–1, where the relative lattice parameters require a counterclockwise rotation of the augite lattice relative to the pigeonite lattice. Of these two we think 1–3 is much more likely, and could be accomplished with reasonable a and c misfits particularly if the two β angles became more similar at high temperature. In order for c_{AUG} sin β_{AUG} to be less than c_{PIG} sin β_{PIG}, c_{AUG} must be considerably less than c_{PIG}. Since there are no "100" augite lamellae in this specimen, but only lamellae of hypersthene parallel to (100), it will not be possible to observe optically the angle of "100" augite lamellae that would be produced by this large negative misfit. If there were, the augite lamellae would be expected to show a pattern that is a combination of 1 and 6 in Figure 5, and would fit in a region of high temperature and low pressure on the hypothetical P–T diagram of Figure 8. This is an appropriate position considering what is known (Wager and Brown, 1968; Lindsley, Brown, and Muir, 1969) about the $P-T$ conditions of the Skaergaard Intrusion.

ACKNOWLEDGEMENTS

The ideas presented in this paper arose from studies of coexisting amphiboles in Massachusetts and southwestern New Hampshire supported by NSF Research Grant GA-467 (to Jaffe and Robinson), studies of pyroxenes from the Hudson Highlands and Adirondacks supported by the New York State Museum and Science Service (Jaffe and Jaffe), general studies of pyroxenes and amphiboles supported by the U. S. Geological Survey, and studies of coexisting amphiboles in Labrador supported by NSF Research Grant GA-11435 (to J. B. Thompson, Jr. and Klein). Stearns A. Morse called the attention of the first author to the optimal phase boundary theory in a different connection. Figure 4 was drafted and the other figures were lettered by Richard Brown. Valuable discussion and suggestions on various aspects of the work were provided by James J. Papike, Charles T. Prewitt, Larry W. Finger, James B. Thompson, Jr., Hans-U. Nissen, Cornelius S. Hurlbut, Jr., and James H. Stout. Versions of the manuscript were reviewed by James J. Papike, Stearns A. Morse, Daniel E. Appleman, Leo M. Hall, and W. Gary Ernst. To each of the above we express our grateful acknowledgement.

References

Bollmann, W., and H.-U. Nissen (1968) A study of optimal phase boundaries: the case of exsolved alkali feldspars. *Acta Crystallogr.* **A24,** 546–557.

Bown, M. G., and P. Gay (1959) The identification of oriented inclusions in pyroxene crystals. *Amer. Mineral.* **44,** 592–602.

———, and ——— (1960) An X-ray study of exsolution phenomena in the Skaergaard pyroxenes. *Mineral. Mag.* **32,** 379–388.

Boyd, F. R., and G. M. Brown (1969) Electron-probe study of pyroxene exsolution. *Mineral. Soc. Amer. Spec. Pap.* **2,** 211–216.

Brown, G. M. (1957) Pyroxenes from the early and middle stages of fractionation of the Skaergaard intrusion, East Greenland. *Mineral. Mag.* **31,** 511–543.

——— (1960) The effect of ion substitution on the unit cell dimensions of the common clinopyroxenes. *Amer. Mineral.* **45,** 15–38.

Burnham, C. W. (1962) Lattice constant refinement. *Carnegie Inst. Year Book* **61,** 132–134.

Deer, W. A., R. A. Howie, and Jack Zussman (1963) *Rock-forming Minerals, Vol.* **2,** *Chain Silicates.* John Wiley and Sons, New York, 379 p.

Jaffe, H. W., and E. B. Jaffe (1971) Bedrock geology of the Monroe quadrangle, New York. *N. Y. State Museum and Sci. Serv., Map and Chart Series No.* **20** (in press).

Jaffe, H. W., Peter Robinson, and Cornelis Klein, Jr. (1968) Exsolution lamellae and optic orientation of clinoamphiboles. *Science* **160,** 776–778.

Klein, Cornelis, Jr. (1964) Cummingtonite-grunerite series: a chemical, optical and X-ray study. *Amer. Mineral.* **49,** 963–982.

——— (1966) Mineralogy and petrology of the metamorphosed Wabush Iron Formation, Southwestern Labrador. *J. Petrology* **7,** 246–305.

——— (1968) Coexisting amphiboles. *J. Petrology* **9,** 282–330.

Kuno, Hisashi, and H. H. Hess (1953) Unit cell dimensions of clinoenstatite and pigeonite in relation to other common clinopyroxenes. *Amer. J. Sci.* **251,** 741–752.

Lindsley, D. H., G. M. Brown, and I. D. Muir (1969) Conditions of the ferrowollastonite-ferrohedenbergite inversion in the Skaergaard Intrusion, East Greenland. *Mineral. Soc. Amer. Spec. Pap.* **2,** 193–201.

———, J. L. Munoz, and L. W. Finger (1969) Unit-cell parameters of clinopyroxenes along the join hedenbergite-ferrosilite. *Carnegie Inst. Year Book* **67,** 91–92.

Morimoto, Nobuo, and Masayasu Tokonami (1969) Oriented exsolution of augite in pigeonite. *Amer. Mineral.* **54,** 1101–1117.

Papike, J. J., Malcolm Ross and J. R. Clark (1969) Crystal-chemical characterization of clinoamphiboles based on five new structure refinements. *Mineral. Soc. Amer. Spec. Pap.* **2,** 117–136.

Poldervaart, Arie, and H. H. Hess (1951) Pyroxenes in the crystallization of basaltic magma. *J. Geol.* **59,** 472–489.

Prewitt, C. T., J. J. Papike, and Malcolm Ross (1970) Cummingtonite, a reversible non-quenchable transition. *Earth Planet. Sci. Lett.* **8,** 448.

Robinson, Peter, and H. W. Jaffe (1969) Chemographic exploration of amphibole assemblages from central Massachusetts and southwestern New Hampshire. *Mineral. Soc. Amer. Spec. Pap.* **2,** 251–274.

———, ———, Cornelis Klein, Jr., and Malcolm Ross (1969) Equilibrium coexistence of three amphiboles. *Contrib. Mineral. Petrology* **22,** 248–258.

Ross, Malcolm, J. J. Papike, and K. W. Shaw (1969) Exsolution textures in amphiboles as indicators of subsolidus thermal histories. *Mineral. Soc. Amer. Spec. Pap.* **2,** 275–299.

———, ———, AND P. W. WEIBLEN (1968) Exsolution in clinoamphiboles. *Science* **159,** 1099–1102.

SMITH, J. V. (1969) Crystal structure and stability of the $MgSiO_3$ polymorphs; physical properties and phase relations of Mg, Fe pyroxenes. *Mineral. Soc. Amer. Spec. Pap.* **2,** 3–29.

SMYTH, J. R. (1970) High-temperature single-crystal X-ray studies of natural orthopyroxenes (abstract). *Amer. Mineral.* **55,** 312.

WAGER, L. R., AND G. M. BROWN (1968) *Layered Igenous Rocks*. Oliver and Boyd, Edinburg and London, 588 p.

WARREN, B. E. (1929) The structure of tremolite, $H_2Ca_2Mg_5(SiO_3)_8$. *Z. Kristallogr.* **72,** 42–57.

WYCOFF, R. W. G. (1968) *Crystal Structures, 2nd Ed., Vol.* 4. Interscience, New York.

ZUSSMAN, JACK (1959) A re-examination of the structure of tremolite. *Acta Crystallogr.* **12,** 309–321.

Manuscript received, August 20, 1970; accepted for publication, December 25, 1970.